Synchronous phase-demodulation of high spatial frequency, concentric-rings, Placido fringe patterns

Manuel Servin

Centro de Investigaciones en Optica A. C., Loma del Bosque 115, 37150, Leon Guanajuato, Mexico.
Author's e-mail: mservin@cio.mx

Abstract: Here a synchronous phase-demodulation method for high spatial frequency (HSF), concentric-rings Placido fringe pattern is proposed. The earliest use of this concentric-rings pattern was to gauge non-spherical irregularities of the human cornea by Portuguese ophthalmologist Antonio Placido in 1880. Most modern corneal topographers use Placido patterns to test human cornea irregularities; a field of application of this paper. Another field of application of HSF conic-carrier fringe patterns is to test wavefronts using what may be called the Placido-Hartmann screen test. These screens would be formed by periodic concentric ring apertures. A Placido-Hartmann test would be sensitive to the radial slope of the wavefront under measurement. Finally as in the Hartmann-Shack test, one may use a radial lenslet array of toroidal-shaped lenses to test the radial slope of a wavefront at the focal plane. The main advantage of estimating the radial slope of a wavefront using a HSF Placido pattern is that a single radial slope image is sufficient to integrate the full wavefront shape.

Keywords (120.5050) Phase measurement; (120.2650) Fringe Analysis.

References

1. T. Schroeder Swartz, R. Mattioli, N. K. Tripoli, D. Horner, and M. Wang, "History," in M. Wang and T. Schroeder Swartz, eds, *Corneal Topography: A Guide for Clinical Application in the Wavefront Era*, 2nd ed., SLACK Inc. (2011).
2. T. Schroeder Swartz, Z. Liu, X. Yang, and M. Zhang, "Topographic Technologies," in M. Wang and T. Schroeder Swartz, eds, *Corneal Topography: A Guide for Clinical Application in the Wavefront Era*, .2th ed., SLACK Inc. (2011).
3. D. Malacara-Doblado and I. Ghozeil, "Hartmann, Hartmann-Shack, and Other Screen Tests," in *Optical Shop Testing*, 3rd ed., D. Malacara ed., John Wiley & Sons, Inc. (2007).
4. L. A, Carvalho and J. C. Castro, "The Placido wavefront sensor and preliminary measurement on a mechanical eye," Optometry and Vision Science, **83**, 108-118 (2006).
5. M. Takeda, H. Ina, and S. Kobayashi, "Fourier-transform method of fringe-pattern analysis for computer based topography and interferometry," J. Opt. Soc. Am, **72**, 156-160 (1982).
6. V. N. Mahajan, "Zernike Polynomials and Wavefront Fitting," in .*Optical Shop Testing*, 3th ed., D. Malacara ed., John Wiley & Sons, Inc. (2007).

1. Introduction

Periodic concentric-ring Placido fringe patterns are commonly used as test image to measure the topography of the human cornea [1]. This radial periodic pattern is widely known as Placido's mire, Placido's target, or Placido's disk and has been used to gauge the human cornea since 1880 [1]. The Placido's target is placed in front of a human eye and its specular reflected image is digitized using a camera placed at a center hole of the Placido's mire. The reflected Placido image is phase-modulated by corneal irregularities of the human eye. Afterwards the reflected (phase-modulated) Placido's mire is phase-demodulated to estimate the radial slope of the corneal topography with respect to its closest sphere [2]. The standard

way to phase-demodulate these Placido targets is first to find the edges of the modulated rings using image processing techniques. Then local radial distances between modulated rings and their reference are estimated at several points. These measured radial distances are proportional to the local radial-slope of the corneal topography deformations. Given that the slope-data is located only at the edges of the rings; this is not a dense data field. In between, no slope-data is collected, masking important and unexpected corneal topography. Finally this sparse local radial-slope data is integrated over the radial coordinate to obtain the topographic deviation of the testing cornea from its closest sphere [2].

As mentioned in the abstract, another use of a Placido pattern would be Hartmann-like test of optical wavefronts. In Hartmann test a two-dimensional (2D) matrix array of holes made into an opaque plate is placed in the propagating path of a wavefront [3]. Then, at a distance d (meters) along the propagating wavefront's path, one takes the image of the shadow cast by the Hartmann screen. This shadow image shows the same hole matrix array but now phase-modulated by the slopes of the testing wavefront in the x and y directions [3]. Then the distance between the center of the Hartmann reference holes and the center of its modulated shadow is taken as an estimation of the local wavefront slope along the x and y directions. These two sets of sparse slope-data are then integrated to obtain the testing wavefront [3]. One may modify the Hartmann set-up, where instead of using a matrix of holes, one uses a Placido target with annular periodic apertures as screen. Then one digitizes at d meters along the wavefront propagation, the Placido target's shadow. By demodulating the Placido's screen shadow one would be able to estimate the radial slope of the measuring wavefront.

Another possible application for synchronous demodulation of HSF Placido rings patterns is the analogous to the Hartmann-Sack test widely used to estimate, for example, the wavefront aberrations of a human eye. In the Hartmann-Shack test, the 2D matrix array of holes is replaced by a 2D matrix of small lenses. The image of the Hartmann-Sack lenslet matrix is then taken at the focal distance of the array [3]. The change from a matrix of small lenses by a periodic array of annular (toroidal) lenses was first proposed by Carvalho et al. [4]. Therefore this may be called the Hartmann-Shack-Carvalho test. This test, as the Placido-Hartmann test would be sensitive to the radial slope of the measuring wavefront.

In this introduction just three examples of possible applications for phase-demodulation of Placido ring patterns were given. But in this paper, the prime interest is on the theoretical aspects of this conic-carrier synchronous phase-demodulation method. We gave these examples just as guiding sample applications of the phase-demodulation method herein proposed.

2. Phase demodulation of high spatial frequency conic-carrier fringe patterns

In this section the theoretical aspects for phase-demodulating high spatial frequency (HSF) conic-carrier Placido fringe patterns is discussed.

Although most Placido reference targets used in digital corneal topographers are binary black-and-white concentric ring patterns, I will model them by the following continuous HSF grey-level fringe pattern

$$\text{Placido}(\rho_1) = 1 + \cos\left(\frac{2\pi}{P}\rho_1\right), \quad \rho_1 = \sqrt{x_1^2 + x_2^2}. \tag{1}$$

Where (x_1, x_2) are the Cartesian coordinates of the Placido test pattern, and $2\pi / P$ is the radial spatial frequency of the conic-carrier or concentric-rings. As mentioned in the introduction, after this HSF reference pattern (Eq. (1)) is reflected by the human cornea and digitized by a CCD camera, the following phase-modulated Placido conic-carrier fringe pattern is obtained,

$$I(\rho,\theta) = a(\rho,\theta) + b(\rho,\theta)\cos\left[\frac{2\pi}{P}\rho + d\,\frac{\partial\varphi(\rho,\theta)}{\partial\rho}\right]. \tag{2}$$

Where d is a real-number which depends on the specific experimental set-up. Polar coordinates (ρ,θ) represent the plane where the modulated Placido image is taken. The background illumination and contrast are respectively $a(\rho,\theta)$, and $b(\rho,\theta)$. Finally $\varphi(\rho,\theta)$ may be either, the corneal topography or the wavefront under test.

The first step towards demodulate a HSF phase-modulated Placido target is to multiply it by the complex-valued Placido's reference. That is, the phase-modulated conic-carrier fringes and the computer-stored reference *must have the same spatial frequency and center.*

$$I(\rho,\theta)\exp\left(i\frac{2\pi}{P}\right)=\left\{a(\rho,\theta)+b(\rho,\theta)\cos\left[\frac{2\pi}{P}\rho+d\,\frac{\partial\varphi(\rho,\theta)}{\partial\rho}\right]\right\}\exp\left(i\frac{2\pi}{P}\rho\right). \quad (3)$$

The cosine signal may be decomposed into its two complex exponential parts, so the left hand side of the above product may be rewritten as,

$$\left\{a+\frac{b}{2}\exp\left[i\left(\frac{2\pi}{P}\rho+d\,\frac{\partial\varphi}{\partial\rho}\right)\right]+\frac{b}{2}\exp\left[-i\left(\frac{2\pi}{P}\rho+d\,\frac{\partial\varphi}{\partial\rho}\right)\right]\right\}\exp\left(i\frac{2\pi}{P}\rho\right). \quad (4)$$

Finally this product may be written as

$$a\,(\rho,\theta)\exp\left(i\frac{2\pi}{P}\rho\right)+\frac{b(\rho,\theta)}{2}\exp\left[i\left(2\frac{2\pi}{P}\rho+d\,\frac{\partial\varphi}{\partial\rho}\right)\right]+\frac{b(\rho,\theta)}{2}\exp\left(-i\,d\,\frac{\partial\varphi}{\partial\rho}\right) \quad (5)$$

Where the 2D polar coordinates (ρ,θ) are shown explicitly. This result is composed by three terms: the first term is the HSF complex reference, amplitude-modulated by the background illumination $a(\rho,\theta)$; the second term is a HSF signal with twice the radial frequency of the reference carrier; finally the third term is the low-frequency (LF), baseband analytical signal that we are looking for. The obtain the baseband signal we apply a low pass filter (LPF) to the signal in Eq. (5) to obtain,

$$\mathrm{LPF}\left\{I(\rho,\theta)\exp\left(i\frac{2\pi}{P}\right)\right\}=\frac{b(\rho,\theta)}{2}\exp\left(-i\,d\,\frac{\partial\varphi(\rho,\theta)}{\partial\rho}\right). \quad (6)$$

Whenever the three spectra in Eq. (5) are well separated we will obtain, error-free, the desired baseband analytical signal. The LPF[.] must be wide enough to pass the spectra of the baseband signal on Eq. (6). On the other hand, the LPF[.] must also reject the two HSF terms on Eq. (5). The condition for spectral separability, and therefore for error-free demodulation, is the following supremum (least upper bound) for the testing slope $\partial\varphi(\rho,\theta)/\partial\rho$,

$$\sup\left[\frac{\partial}{\partial\rho}\left(d\,\frac{\partial\varphi(\rho,\theta)}{\partial\rho}\right)\right]<\frac{2\pi}{P}. \quad (7)$$

The final step to obtain the desired radial slope $\partial\varphi(\rho,\theta)/\partial\rho$ is,

$$\frac{\partial\varphi(\rho,\theta)}{\partial\rho}=\frac{-1}{d}\tan^{-1}\left[\frac{\mathrm{Im}\left\{\ \mathrm{LPF}[\ I(\rho,\theta)\exp\left(i2\pi\rho/P\right)\ ]\ \right\}}{\mathrm{Re}\left\{\ \mathrm{LPF}[\ I(\rho,\theta)\exp\left(i2\pi\rho/P\right)\ ]\ \right\}}\right]. \quad (8)$$

Where Im[.] and Re[.] are operators which take the real and imaginary parts of their argument. Eq. (8) gives in a single formula, the proposed synchronous HSF, conic-carrier, phase-demodulation algorithm. The estimation in Eq. (8) is dense, that is we obtain slope-estimation at every pixel on the measuring field, not only at the ring edges. Of course the phase in Eq. (8)

is wrapped modulo 2π, so you will need to unwrap it before radial integration to obtain the desired wavefront or topography $\varphi(\rho,\theta)$.

3. An illustrative computer generated example

In this section an example of the HSF conic-carrier phase-demodulation method is presented to better understand the details of the proposed technique.

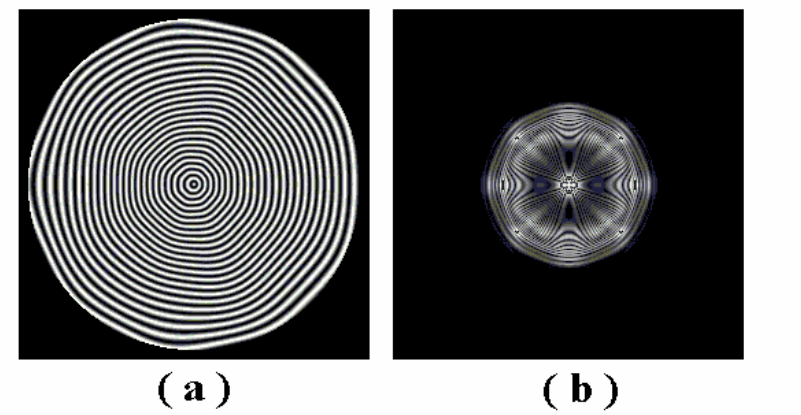

Figure 1. This figure shows a phase-modulated Placido HSF conic-carrier fringe pattern. Panel (a) shows the phase-modulated Placido target in Eq. (2). Panel (b) shows the spectrum of the modulated Placido target in panel (a).

Figure 1 shows a phase-modulated Placido target and the magnitude of its frequency spectrum. Panel 1(a) is the phase-modulated HSF conic-carrier Placido fringe pattern. This example was carried out using low, 256x256 pixel images to clearly show the phase modulation on the HSF ring fringes. The spatial frequency of the conic-carrier is 0.4π radians/pixel along the radial axis ρ. Panel 1(b) shows the magnitude of the Fourier spectrum of the modulated fringes in panel 1(a). Panel 1(b) shows that both, the positive and negative complex phase-modulated spectra are superimposed at the donut-shaped region with radius of 0.4π (Eq. (2)). So these two complex cosine components cannot be separated by spectral shift as in the case of synchronous linear-carrier interferometry [5]. This is a very important difference between using a phase-plane [5] (or linear-carrier) or a conic-carrier. Using a phase-plane as carrier the two conjugate spectra are already separated, while in conic-carrier it is not obvious at all (until this paper) how to separate the two conjugate signals. The only thing in common between linear and conic synchronous interferometry, is the use of a synchronous carrier; in one case a phase-plane and in the other a phase-cone.

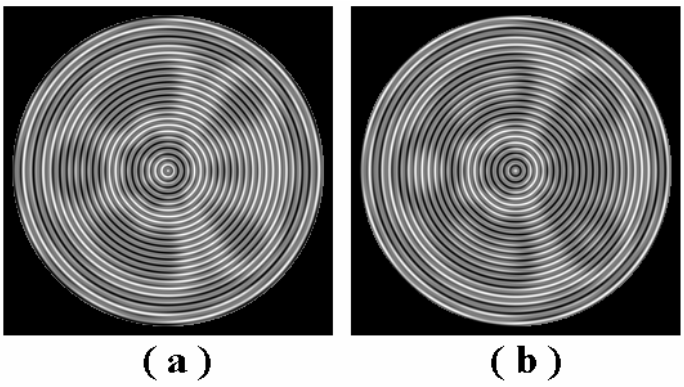

Figure 2. This figure shows the real and the imaginary parts of the product in Eq. (3). Panel (a) shows the real part of the product, while panel (b) the imaginary part.

Figure 2 shows the real and imaginary parts of the product in Eq. (3). We may see, as expected, that the real (panel 2(a)) and the imaginary parts (panel 2(b)) are in quadrature.

Figure 3 shows in panel 3(a) the frequency spectrum of the product in Eq. (3-5). And panel 3(b) depicts the demodulated (wrapped) phase-slope according to the synchronous conic-carrier demodulation proposed (Eq. (8)).

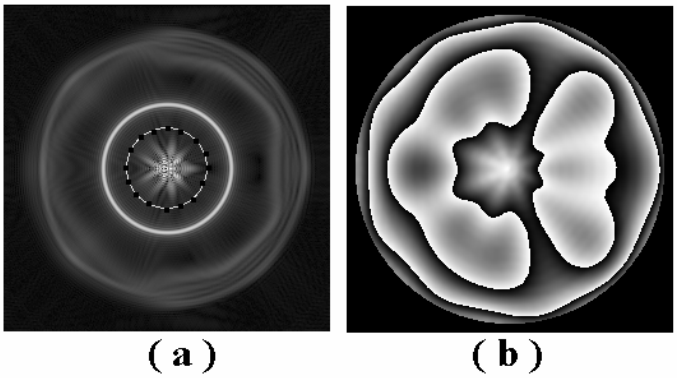

Figure 3. Panel (a) shows the spectrum of the phase-modulated Placido target multiplied by the complex reference Eq. (3-5). Panel (a) also shows the size of the LPF[.] as a dotted ring between the desired baseband analytical signal, and the conic-carrier reference. Panel (b) shows the wrapped phase modulo 2π after applying the LPF[.] in panel (a), and inverse Fourier transforming the spectrum inside the LPF[.] dotted ring.

Panel 3(a) depicts the three spectral components of the signal in Eq. (5). The spectrum at the origin is the baseband term; the desired analytical signal (the third term in Eq. (5)). The middle-frequency spectrum (the first term in Eq. (5)) has the same spatial frequency as the conic reference: $\omega_\rho = 0.4\pi$ radians/pixel. Finally the outermost spectral "halo" (the middle term in Eq. (5)) has a conic-carrier of twice the reference signal: $\omega_\rho = 0.8\pi$ radians/pixel. Panel 3(a) depicts as a dotted circle the boundary of the LPF[.] used in this simulation. The LPF[.] let pass only the full spectrum of the baseband analytical signal.

4. Generalization and limitations of the synchronous conic-carrier method

This method may be readily generalized to *n*-dimensions in the Euclidean space. We may simply assume that the radial coordinate is now given by

$$\rho_1 = \sqrt{x_1^2 + x_2^2 + ... + x_n^2} \tag{8}$$

That is because no explicit mention to the dimensions of the radial coordinate ρ was needed. So the results obtained are already in the *n*-dimensional Euclidian space. For example in three dimensions the Placido target is formed by concentric spheres.

The main advantage of estimating the radial-slope $\partial\varphi(\rho,\theta)/\partial\rho$ of a smooth function (wavefront or topography) is that full recovery of $\varphi(\rho,\theta)$ is possible. That is because in a circular (or annular) unit pupil any continuous smooth function may be represented by a complete set of orthonormal Zernike circle (or annular) polynomials as [6],

$$\varphi(\rho,\theta) = \sum_{j=1}^{\infty} a_j Z_j(\rho,\theta) \tag{9}$$

Where expansion a_j coefficients are given by [6],

$$a_j = \frac{1}{\pi}\int_{\rho=0}^{1}\int_{\theta=0}^{2\pi}\varphi(\rho,\theta)Z_j(\rho,\theta)\;\rho\;d\rho\;d\theta \tag{10}$$

The radial derivative of any Zernike circle polynomials $Z_j(\rho,\theta)$ is always non-zero for all $j \in \mathbb{N}$ [6], that is,

$$\frac{\partial Z_j(\rho,\theta)}{\partial \rho} \neq 0\,, \quad \forall\,(j \in \mathbb{N})\,. \tag{11}$$

As a consequence we only need a spatially-dense estimation of the radial slope to obtain all the details of the testing wavefront or topography $\varphi(\rho,\theta)$. In contrast the Hartmann, or Hartmann-Sack tests, need several slope-images along each Cartesian coordinates. The proposed HSF conic-carrier phase-demodulation method gives such required, dense-slope estimation over the measuring field.

The main limitation of the conic-carrier phase-demodulation method is that the center of the modulated Placido target must exactly coincide with the center of the complex reference computer-stored conic carrier Eq. (3). Otherwise a decentering phase-error between the conic-carrier's reference and the modulated one would arise, giving a spurious demodulated phase.

4. Conclusions

A method for synchronous phase-demodulation of high spatial frequency (HSF) conic-carrier Placido fringe patterns was developed. With the proper experimental set-up, this Placido fringe demodulation method may estimate spatially-dense radial slope. The main advantage of spatially-dense estimation is that a single slope-image is needed to fully integrate the testing variable. In contrast, using a Hartmann screens (a matrix of holes), one needs two slope data along the *x* and *y* directions to fully estimate the wavefront under test. Moreover, today most slope measuring methods (using Placido, Hartmann or Hartmann-Shack screens) provide 2D sparse slope estimations. This fact may hide unexpected features of the measuring slope among these sparse collecting data points. On the other hand, using synchronous conic-carrier demodulation, one estimates the radial-slope at every pixel inside the area of interest. We also mentioned in the introduction, for motivation purposes only, some applications of modulated Placido fringe patterns. Archetypal applications are: corneal topography, eye wavefront aberrometry and large telescope mirror testing. However our main interest in this paper was to present the theoretical aspects of this synchronous HSF conic-carrier phase-demodulation method independently of the applications it may have.

Finally we want to mention that the Placido fringe analysis method described herein is patent pending at the United Stated Patent and Trade Mark Office (USPTO).

Acknowledgements
I want to acknowledge the financial support of the Mexican Council of Technology (Consejo Nacional de Ciencia y Tecnologia CONACYT).